

## Repurposing tofacitinib as an anti-myeloma therapeutic to reverse growth-promoting effects of the bone marrow microenvironment

Christine Lam,<sup>1,2</sup> Ian D. Ferguson,<sup>1,2</sup> Margarette C. Mariano,<sup>1,2</sup> Yu-Hsiu T. Lin,<sup>1,2</sup> Megan Murnane,<sup>2,3</sup> Hui Liu,<sup>1,2</sup> Geoffrey A. Smith,<sup>4</sup> Sandy W. Wong,<sup>2,3</sup> Jack Taunton,<sup>4</sup> Jun O. Liu,<sup>5</sup> Constantine S. Mitsiades,<sup>6</sup> Byron C. Hann,<sup>2</sup> Blake T. Aftab<sup>2,3</sup> and Arun P. Wiita<sup>1,2,\*</sup>

<sup>1</sup>Department of Laboratory Medicine, University of California, San Francisco, CA; <sup>2</sup>Helen Diller Family Comprehensive Cancer Center, University of California, San Francisco, CA; <sup>3</sup>Department of Medicine, University of California, San Francisco, CA; <sup>4</sup>Department of Cellular and Molecular Pharmacology, University of California, San Francisco, CA; <sup>5</sup>Department of Pharmacology and Molecular Sciences, Johns Hopkins School of Medicine, Baltimore, MD and <sup>6</sup>Department of Medical Oncology, Dana-Farber Cancer Institute, Boston, MA, USA

©2018 Ferrata Storti Foundation. This is an open-access paper. doi:10.3324/haematol.2017.174482

Received: June 12, 2017.

Accepted: March 15, 2018.

Pre-published: April 5, 2018.

Correspondence: arun.wiita@ucsf.edu

---

## **Supplementary Materials**

### **Repurposing tofacitinib as an anti-myeloma therapeutic to reverse growth-promoting effects of the bone marrow microenvironment**

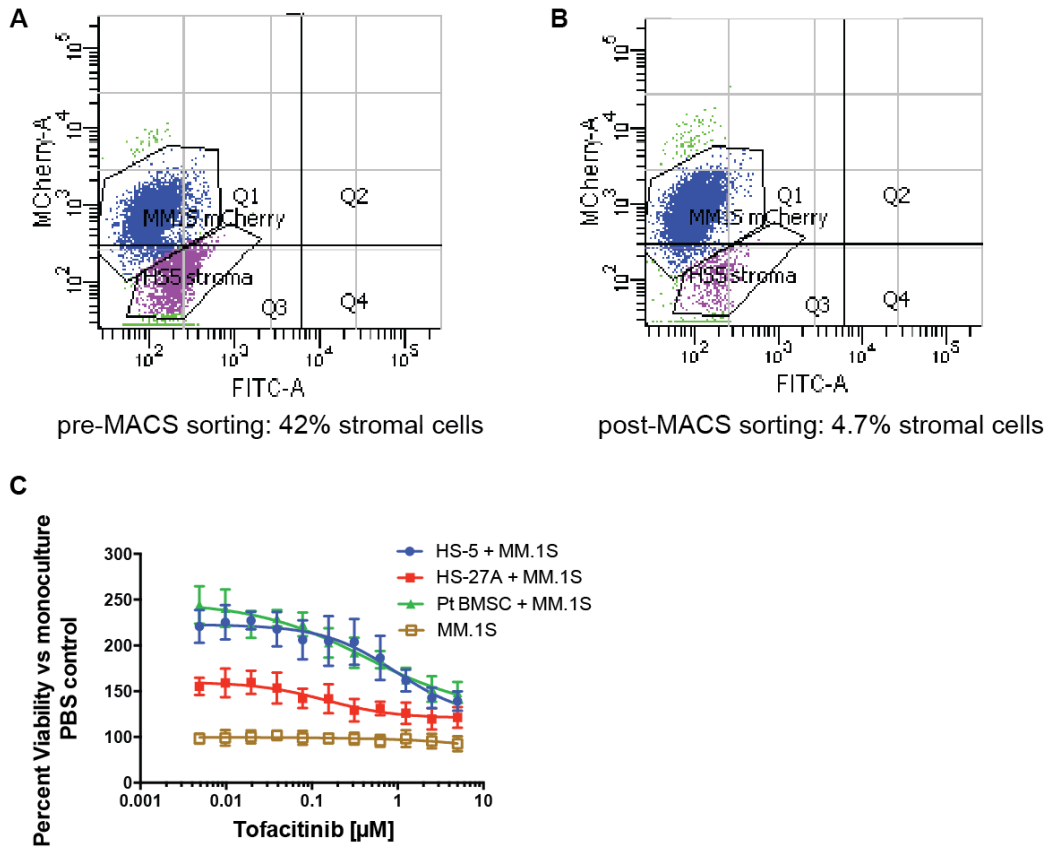
#### **Contents:**

Supplementary Figures 1-6

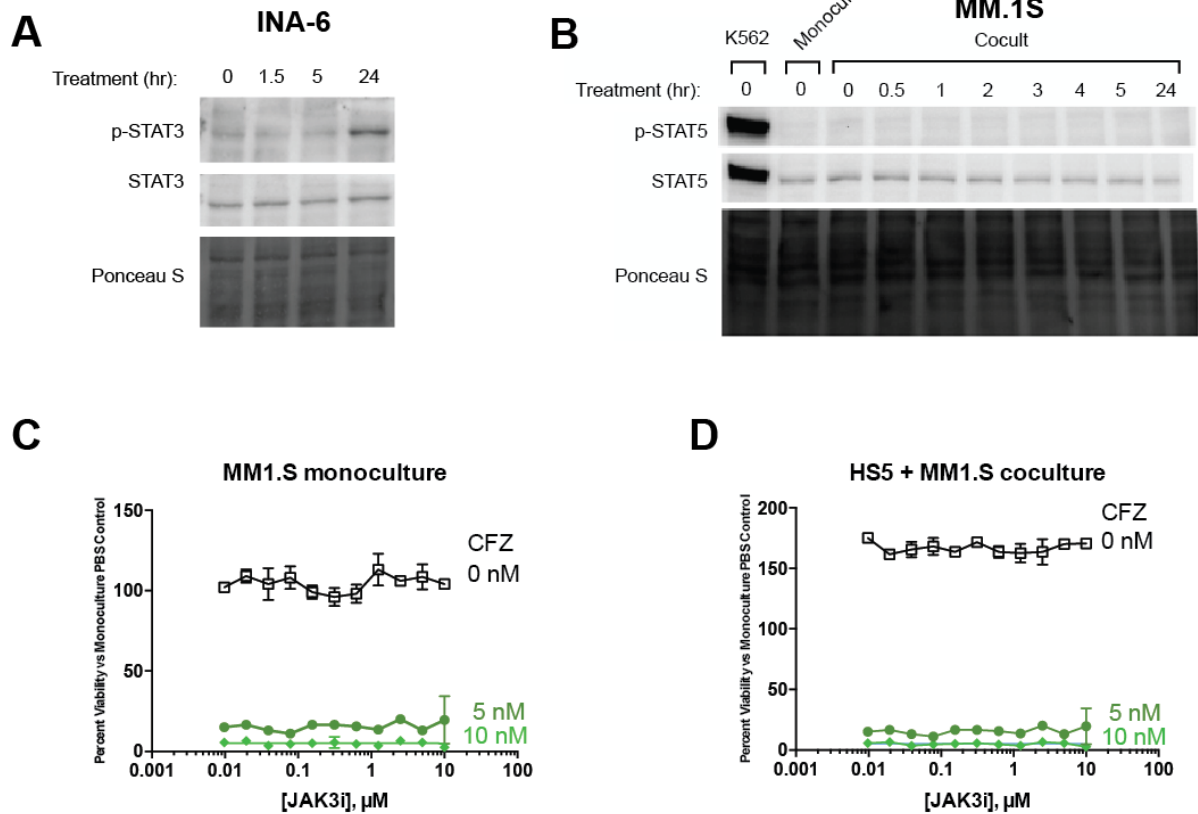
Supplementary Methods

Supplementary Datasets 1-2

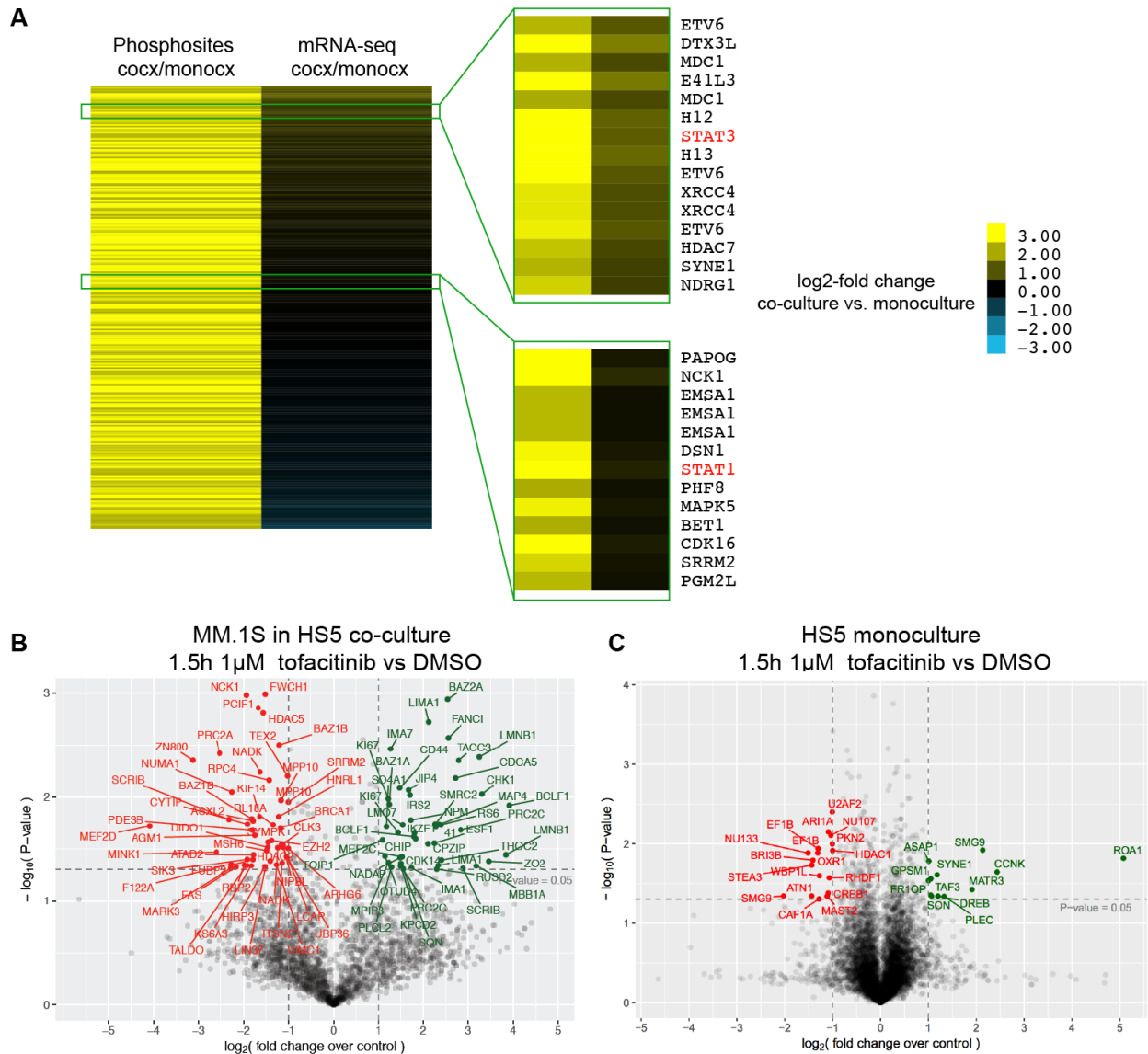
Supplementary References



**Supplementary Figure 1. Sample preparation for RNA-seq and tofacitinib treatment with primary patient stroma.** After 24 hr of co-culture with HS5 stromal cells, 10E6 MM.1S cells were harvested by scraping and separated from stromal cells by Accutase (Sigma) treatment. mCherry- and luciferase-labeled MM.1S cells were enriched by CD138+ magnetic beads prior to RNA-seq library preparation. **A.** Flow cytometry of cells pre-magnetic bead selection and **B.** post-magnetic bead selection demonstrates significant enrichment of the mCherry-positive MM.1S sample used for RNA-seq, with number of stromal cells decreased from 42% pre-sorting to 4.7% after sorting. **C.** Replicate assay of tofacitinib treatment of MM.1S (as in Fig. 1A) with inclusion of low-passage bone marrow stromal cells derived from a primary patient sample.

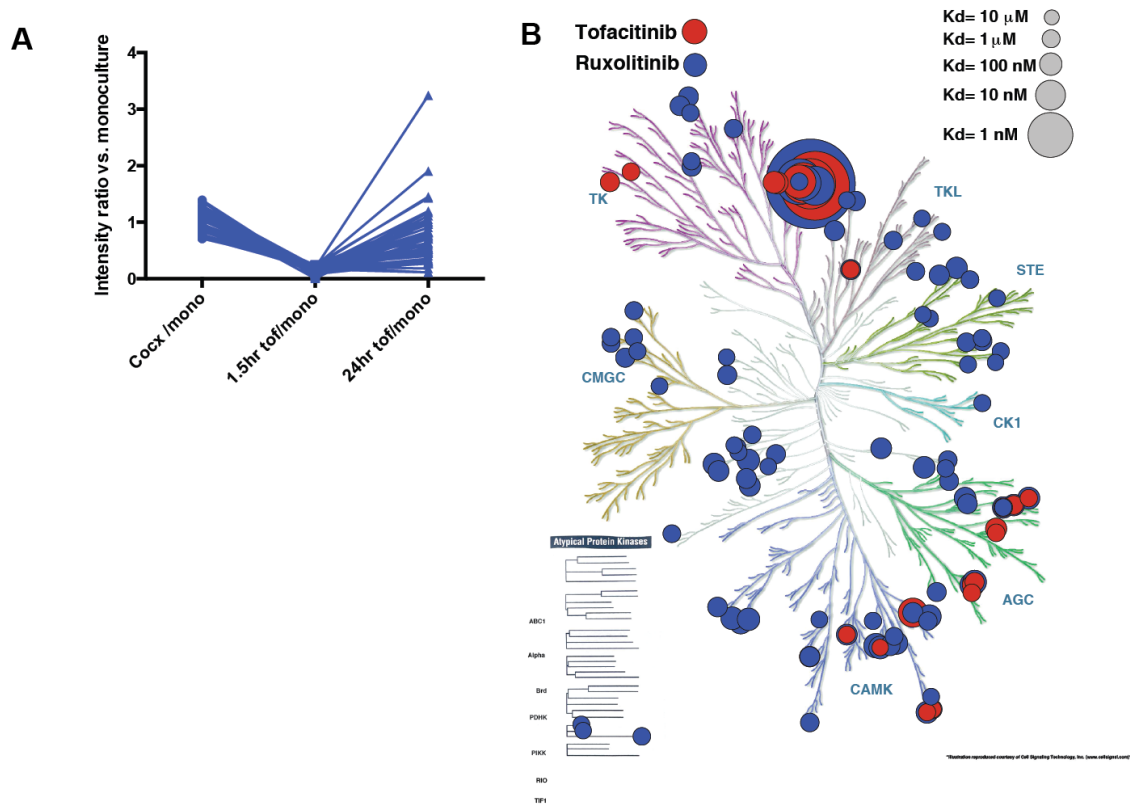


**Supplementary Figure 2. STAT5 and JAK3 do not appear to play a major role in stromal-induced proliferation in MM.** **A.** Western blotting of IL-6 dependent cell line INA-6 shows limited STAT3 phosphorylation at baseline which is decreased by tofacitinib and then leads to rebound phosphorylation at 24h, as seen for MM.1S (Fig. 3A). **B.** STAT5 phosphorylation is undetected in MM.1S cells in monoculture or co-culture with HS5. A sample from the cell line K562 is included as a positive control for antibody performance, as it is known to have strong induction of STAT5 signaling. **C.-D.** JAK3i does not show any prominent synergy with carfilzomib (CFZ) treatment of MM.1S in monoculture or co-culture. Error bars represent +/- S.D. from CellTiterGlo assay performed in quadruplicate in 384-well plates.

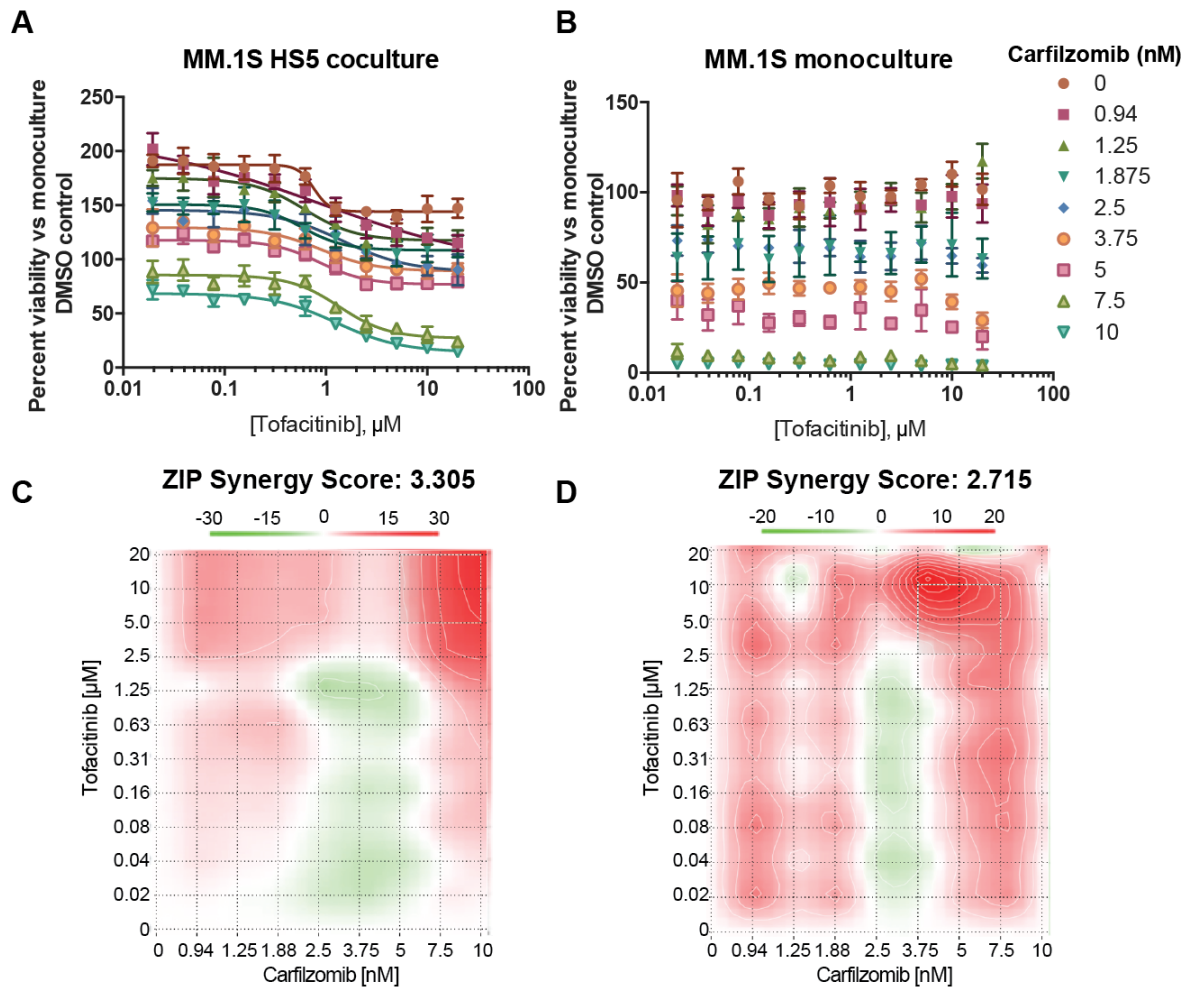


**Supplementary Figure 3. Phosphoproteomic changes in co-culture are driven by signaling rather than protein abundance changes.** A. Heatmap of all 544 upregulated phosphosites, showing log<sub>2</sub> fold-change >2 in MM.1S untreated coculture with HS5 vs. monoculture, compared with log<sub>2</sub>-fold change by mRNA-seq for the genes encoding the phosphoproteins, demonstrates that the phosphosite intensity changes are largely driven by changes at the post-translational modification level and not by changes in transcript or protein abundance. Insets demonstrate greatly increased phosphorylation on STAT3 and STAT1 (red) in co-culture

compared to smaller increases at the mRNA level, consistent with phosphorylation and total protein expression changes seen by Western blotting (Fig. 3). **B.** Volcano plot showing log<sub>2</sub>-fold change (x-axis; positive values indicate increased phosphorylation, negative values indicate decreased) and significance (y-axis;  $-\log(10) p$ -value by *t*-test) for phosphopeptides in MM.1S cells in co-culture with HS5 stromal cells after 1.5 hr of 1 uM tofacitinib versus DMSO control ( $n = 2$ ). Cutoffs for significance are  $\pm 1$  on log<sub>2</sub>-fold scale and  $p < 0.05$  (down-regulated labeled in red; upregulated in green). **C.** Similar analysis for HS5 stromal cells in monoculture ( $n = 2$ ; 7345 quantified phosphopeptides) demonstrates many fewer significantly-changed phosphopeptides, consistent with lack of viability effects of tofacitinib treatment in this cell line (Fig. 1B).

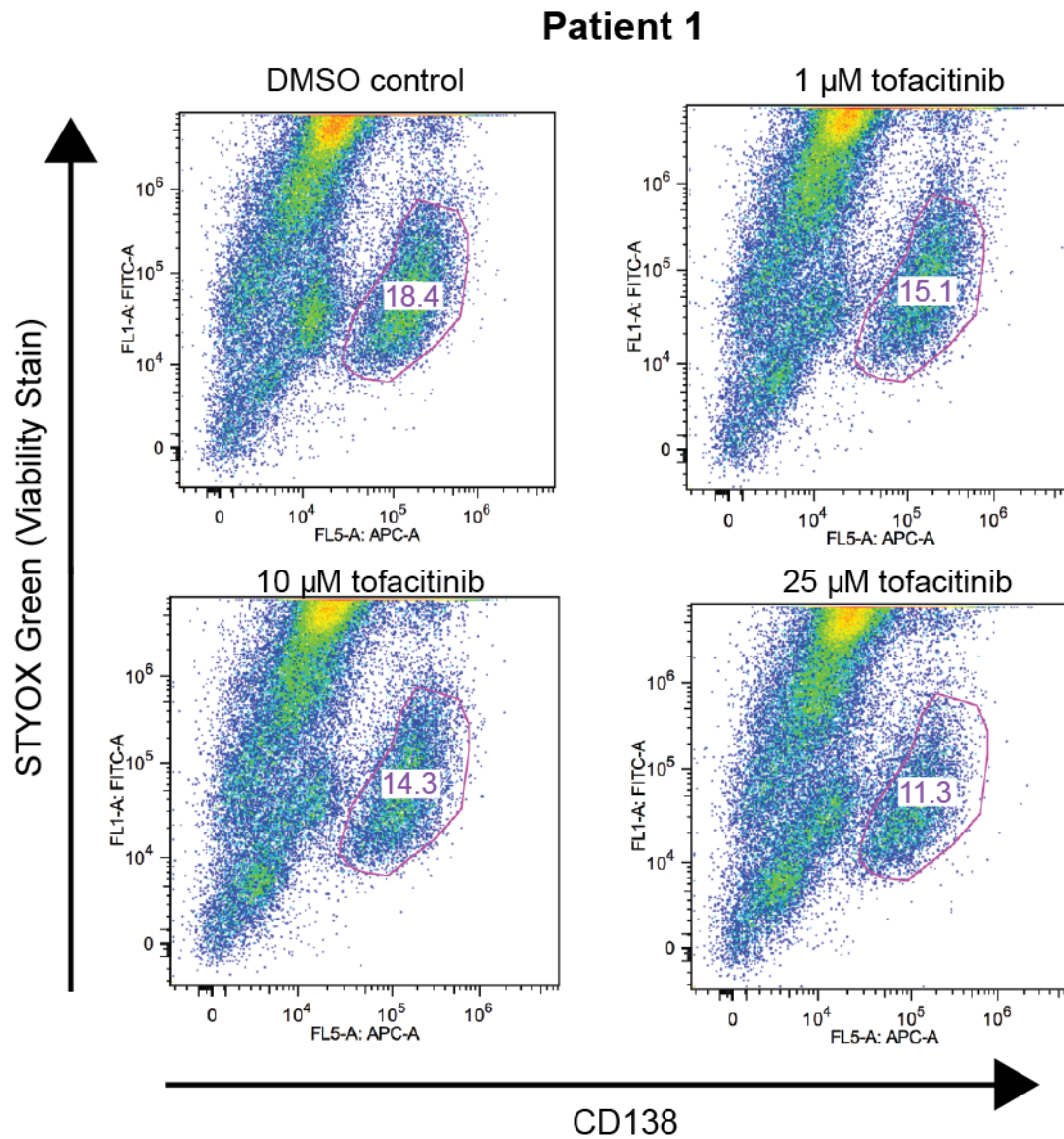


**Supplementary Figure 4. Phosphoproteomics does not reveal specific tofacitinib off-target effects in MM. A.** Only 54 phosphopeptides were identified that met the criteria: 1) <50% intensity change in untreated co-culture vs. monoculture and 2) decreased >4-fold after 1.5 hr tofacitinib treatment. These phosphopeptides showed no significant biological pathway enrichment upon Panther or other bioinformatic analysis by Enrichr, revealing no prominent off-target effects of tofacitinib by this analysis. **B.** Cell-free kinase inhibitor activity data from LINCS KINOMEscan database demonstrates that tofacitinib is much more specific for JAK-family kinases (large circles, denoting strong binding, top center) than ruxolitinib, which has off-target activity against many more kinases. Figure rendered using KinomeRender (Chartier *et al. PeerJ* (2013) 1:e126).



**Supplementary Figure 5. Tofacitinib shows weakly synergistic effects with carfilzomib in MM.1S cells.** **A.-B.** Treatment was performed sequentially with 24h of tofacitinib followed by 24h of carfilzomib at specified doses. **C.-D.** For combination matrices, the interaction landscapes are shown in 2D plots. As in Fig. 6, the ZIP method is used to calculate synergy across the landscape (red = positive score, synergistic, green = negative score, antagonistic) as well as calculate an overall synergy score  $\delta$ , the difference in percentage inhibition compared with the expected additive compound effect. Both coculture and monoculture results demonstrate overall mild synergy ( $\delta$  score <4) with some areas of potential antagonism. Note different scale bars on each 2D landscape output from ZIP. Error bars represent +/- S.D. from CellTiterGlo assay performed in quadruplicate in 384-well plates.





**Supplementary Figure 6. Flow cytometry data of MM patient plasma cells treated *ex vivo* by tofacitinib.** Example raw data shown for one replicate of primary patient sample (Patient 1) quantified in Fig. 7. CD138+ viable MM patient-derived plasma cells (viability measured as lack of staining by SYTOX green stain) were gated and quantified as a percentage of all recorded singlets in the sample. Tofacitinib treatment was for 24 hr after co-incubation with 50 ng/mL IL-6 for 17 hr prior to treatment.

## **Supplementary Methods**

### *Cell Culture Conditions*

HS5 and HS27A stromal cell lines and U266 MM cell line were obtained from American Type Culture Collection (ATCC). MM.1S mC/Luc, stably expressing mCherry and luciferase, were generated from parental MM.1S line obtained from ATCC, as previously described<sup>1</sup>. Stromal cells from a primary myeloma patient aspirate were derived as described<sup>2</sup>. The RPMI8266 mC/Luc, and JJN3 mC/Luc lines were generated from parental cell lines obtained from the Deutsche Sammlung von Mikroorganismen und Zellkulturen (DSMZ) repository. AMO-1 cells were kindly provided by Dr. Cristoph Driessen at Kantonsspital St. Gallien, Switzerland. These cell lines were stably transduced with a lentiviral expression plasmid constitutively expressing luciferase and mCherry, generated and kindly provided by Dr. Diego Acosta-Alvear at UCSF. L363 cell line was also obtained from DSMZ. KMS11 cells were obtained from JCRB Cell Bank. INA-6 cells were obtained from Dr. Renate Burger at University Hospital Schleswig-Holstein, Germany. All recombinant cytokines were obtained from ProSpec.

### *RNA-seq*

All cells were harvested by Accutase incubation for 10 min at 37 C to separate MM.1S from HS5 into a single-cell suspension. Cells were then separated using CD138+ MicroBeads (Miltenyi) on a Miltenyi MidiMACS system. RNA-seq performed on HS5 stromal cells alone further allowed for filtering of highly expressed stromal cell genes that could interfere with analysis of MM.1S cells in co-culture even at <5% contamination.

### *Western Blot Analysis*

For co-culture studies,  $3 \times 10^5$  HS5 were seeded into 6 well plate. 17 hours later,  $5 \times 10^6$  MM.1S mC/Luc cells were added on top of stromal cell layer. For monoculture studies  $5 \times 10^6$  MM.1S cells alone were used. Cells were treated with tofacitinib or ruxolitinib from 0-24 hours and the supernatant, containing all MM.1S cells in suspension, harvested for processing by centrifugation. All Western blots were performed at in biological duplicate with representative blots displayed. pSTAT3 (Tyr705), STAT3, pSTAT1 (Tyr701)(58D6), STAT1, pJAK1(Tyr1022/1023), JAK1, pJAK2 (Tyr1008), JAK2, pJAK3 (Tyr980/981), JAK3, pTYK2 (Tyr1054/1055), pSTAT5 (Tyr694), and STAT5 antibodies were purchased from Cell Signaling Technology. Tyk2 antibody was purchased from Santa Cruz Biotechnology. Western blot was carried out as previously described<sup>3</sup>.

#### *Liquid Chromatography-tandem mass spectrometry phosphoproteomics*

Spectra were acquired in data-dependent acquisition mode at 70,000 resolution. Raw mass spectrometry data for two biological replicates were processed using Maxquant v1.5 (ref. 4) versus the Uniprot human proteome (downloaded Feb. 20, 2017; 157,537 entries), with phospho (STY) selected as a fixed modification and match between runs enabled. Only phosphopeptides with measured MaxQuant MS1 intensity in all samples were used for analysis. Median intensity normalization of all phosphopeptides in the sample was performed prior to analysis.

**Supplementary Dataset 1 (attached as Excel file).** DESeq output for RNA-seq comparing MM.1S monoculture vs. MM1.S in co-culture with HS5 stromal cells.

**Supplementary Dataset 2 (attached as Excel file).** MaxQuant output for phosphoproteomic data used for analysis.

## Supplementary References

1. McMillin DW, Delmore J, Weisberg E, et al. Tumor cell-specific bioluminescence platform to identify stroma-induced changes to anticancer drug activity. *Nat Med.* 2010;16(4):483-489.
2. Ramakrishnan A, Torok-Storb B, Pillai MM. Primary marrow-derived stromal cells: isolation and manipulation. *Meth Mol Biol.* 2013;1035(75-101).
3. Wiita AP, Ziv E, Wiita PJ, et al. Global cellular response to chemotherapy-induced apoptosis. *eLife.* 2013;2(e01236).
4. Cox J, Mann M. MaxQuant enables high peptide identification rates, individualized p.p.b.-range mass accuracies and proteome-wide protein quantification. *Nat Biotechnol.* 2008;26(12):1367-1372.